Characterization and FTIR spectral studies of human urinary stones from Southern India

E.V. Wilson [a], M. Junaid Bushiri [b,*], V.K. Vaidyan [a]

[a] Centre for Advanced Research in Physical Sciences, Department of Physics, Fatima Mata National College, Kollam 691 001, Kerala, India
[b] Department of Physics, Cochin University of Science and Technology, Kochi 682 022, Kerala, India

ARTICLE INFO

ABSTRACT

Urinary stones resected from urinary bladders of patients hailing from Kollam district of Kerala State, India were analyzed by SEM, XRD and by thermal analysis techniques. The analytical results indicate that, stones have different composition, i.e., calcium phosphate, calcium phosphate hydroxide and sodium calcium carbonate. Infrared spectral studies also reveal the presence of phosphates or carbonates in these samples. Further, IR spectral investigations have revealed that amorphous carbonated species are occupied in PO_4 sites in calcium phosphate type stone and OH sites in calcium phosphate hydroxide sample. Thermal studies of these samples also reveal that, carbon dioxide is released from carbonated samples upon heating which is related to amount of carbon content and bond strength. Crystals with defects and irregular morphology are grown inside the urinary bladder due to variation in crystal growth conditions.

1. Introduction

Kidney stones, is a most painful and prevalent urological disorders of the urinary system since prehistoric period [1,2]. The increasing incidence of crystal deposition diseases such as urinary stones, kidney stones, gall stones, gout, etc., in people of all ages affecting a considerable number of the total population is a major social and economic problem, considering the number of days lost from work and cost of hospitalization [3–5]. Nephrolithiasis or kidney stones are small hard crystals formed when uric acid or calcium, magnesium, ammonium ions phosphates, carbonate or oxalate precipitate out of urine and build up on the inner surface of kidney [2]. Urinary calculus is a multiphase material and its compositions are complex and diverse containing inorganic crystals and organic matrix and majority is made up of calcium oxalate or other compounds of calcium [2]. In urinary calculi containing more than one mineral, the inorganic fraction is arranged in concentric layers of abruptly differing composition around a common nucleus. One interesting feature of such stones is that their centre usually consists of different forms of calcium phosphate. These include hydroxyapatite, $Ca_{10}(PO_4)_6(OH)_2$, also known as basic calcium hydrogen phosphate, and rarely brushite, calcium hydrogen phosphate dehydrate [7]. Apart from this amorphous carbon or carbonate species or different types of proteins may likely to attach with urinary stones. The morphology and chemical composition depend on supersaturation and chemical reaction pathway in nucleation mediums with varying pH [5]. The structural and composition analysis of these stones are more complicated due to the formation of multiple phases having same chemical formulae or combination of different constituents. The qualitative and quantitative knowledge of composition of urinary calculi may help for understanding their etiology and for the development of prophylactic measures planning future strategy for the effective treatment of similar diseases [6]. Analytical methods such as XRD, SEM and FTIR can provide vital information regarding chemical and structural information of urinary calculi to a certain extent. In the present study, urinary stones resected from urinary bladder of some patients hailing from Kollam district of Kerala State, India are analyzed and characterized.

2. Experimental

Stones resected from urinary bladders were washed several times in water and ethanol and kept it for a period of about a month for in air atmosphere at room temperature ($30\,°C$) before doing analytical measurements. 2A FEI Quanta 200F was used to record SEM. Philips PW1840 X-ray diffractometer with Cu Kα radiation ($1.5406\,\text{Å}$) was used for taking diffraction pattern of the well crushed and powdered samples. FTIR spectrum of the sample was recorded using Bruker IFS 66 v FTIR in the wavenumber range 400–$4000\,\text{cm}^{-1}$ with a resolution better than $3\,\text{cm}^{-1}$ by KBr pellet method. DTA/TG curves of the samples in the present investigation

* Corresponding author. Tel.: +91 9495348631.
E-mail address: junaidbushiri@gmail.com (M.J. Bushiri).

Table 1
d-values of the urinary stone samples with JCPDS data.

Sample 1 d-value (Å)		Sample 2 d-value (Å)		Sample 3 d-value (Å)	
Observed	JCPDS 09-0169 $Ca_3(PO_4)_2$	Observed	JCPDS 09-0432 $Ca_5(PO_4)_3(OH)$	Observed	JCPDS 06-0513 $Na_2Ca(CO_3)_2$
2.79	2.88	2.80	2.81	2.74	2.63
2.67	2.61	2.73	2.72	3.58	3.03
3.42	3.21	2.77	2.78	5.77	5.26

were taken using a STAR TGA/SDTA851 with a temperature accuracy of $\pm 0.25\%$ in the temperature range of 25–800 °C. Differential scanning calorimetric studies were carried out on a Mettler Toledo system using a sample mass of approximately 0.92 g and a scan rate of 0.5 degree per minute. Samples collected from different patients are grouped into three types, which are named as sample 1, sample 2 and sample 3 for the rest of the discussion.
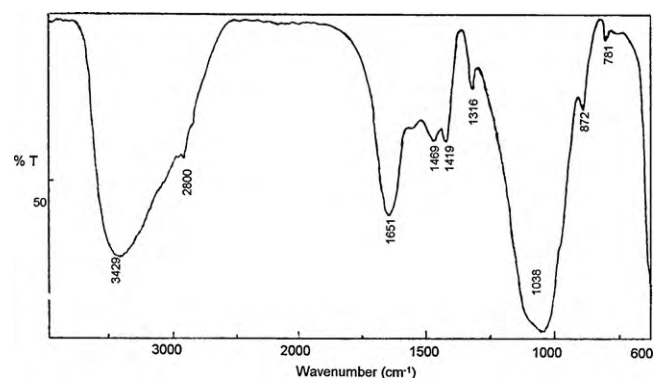
3. Results and discussion

XRD patterns of the samples under investigation are analyzed, the 'd' values of sample 1 are compared with standard 'd' values from JCPDS data (Table 1) [8]. The XRD pattern of sample 1 can be indexed to that of Calcium phosphate $Ca_3(PO_4)_2$, (JCPDS 09-0169) which is known to crystallize in rhombohedral system. For sample 2, XRD peaks can be indexed to those of calcium phosphate hydroxide (JCPDS 09-0432) with hexagonal crystalline structure [8]. The observed XRD peaks of sample 3 indicate that this compound mostly contain sodium calcium carbonate (JCPDS-06-0513) and is known to crystallize in hexagonal system.

The information obtained from the infrared spectral pattern of samples 1 and 2 is given in Table 2. Studies on the phosphates containing PO_4^{3-} ion indicate that the stretching and bending vibrations occur in the frequency regions 900–1200 and 300–600 cm^{-1} respectively [9]. Strong and broad IR band extending from 985 to 1100 cm^{-1} observed in sample 1 with intense feature at 1038 cm^{-1} is due to PO_4^{3-} stretching vibration (Fig. 1) [9–18]. The sharp and intense peak in the spectrum occurs at 605 cm^{-1} may be due to the bending vibration of PO_4^{3-} [9–11]. The breakdown of urea in human urine leads to the formation of high carbon dioxide content, eventually this will converted in to amorphous carbon or carbonate species which may attach to urinary stones [17]. When the planar carbonate substitutes randomly on the phosphate tetrahedron, the apatite lattice symmetry is modified and consequently the observed vibrational bands are modified and additional bands may appear. The local environments are modified by the creation of vacancies and/or substitutions leading to different vibrational frequencies and bandwidths. The IR spectral pattern of sample 2 is almost identical that of sample 1 with slight change in peak positions (Fig. 2) and an additional band is observed at 1995 cm^{-1} may
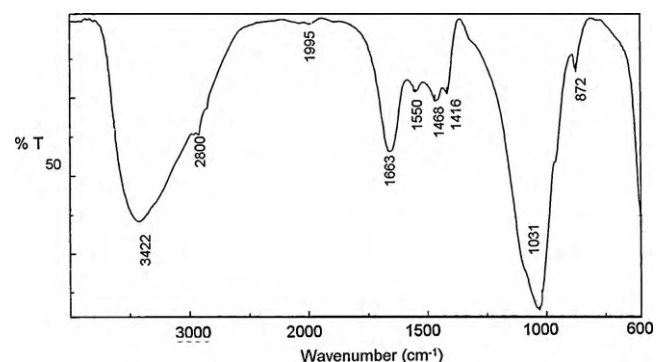

Fig. 1. FTIR spectrum of the sample 1, in the range 400–4000 cm^{-1}.

be due to adsorbed CO vibrations. Carbonate ions can also be incorporated at the surface of the calcium phosphate type crystals and sometimes it may be in amorphous form [19]. In calcium phosphate type crystals, carbonate (CO_3) ion is preferred to substitute in PO_4 site rather than in OH site which gives IR absorption band at 872 cm^{-1} [17]. In the present study, sample 1 shows moderately intense band at 1419 and at 1469 cm^{-1} while in sample 2, a weak band at 1416 and moderately intense at 1468 cm^{-1} and are contributed to CO_3 ion [19]. Apart from this, a weak band observed at 1550 cm^{-1} in sample 2 further confirms the presence of carbonates groups substituted in OH sites [16]. Strong and broad band extending from 3250 to 3520 cm^{-1} with a peak at 3429 and a shoulder at 2800 cm^{-1} which arises due to the stretching of O–H functional group [3,9,14,20]. Moderately strong absorption peak at 1651 cm^{-1} is assigned to the deformation of OH group [3,9]. The C=C vibration from amorphous carbon also contribute to band at 1550 cm^{-1}.

Unlike the other two samples, the sample 3 contains mainly carbonate functional group as inferred from the XRD pattern described previously. The weak band at 883 cm^{-1} corresponds to stretching vibration of CO_3^{2-} ion which is situated in monovalent anionic sites of the apatite structure (Fig. 3) [21,22,17]. The weak bands at 1034 and 1093 cm^{-1} may be assigned to C–O stretching vibrations, while one of strongest band in the spectrum at 1620 cm^{-1} assigned to OH bending vibrations (Table 3).

Table 2
IR spectral data (cm^{-1}) of urinary stone sample 1 and sample 2.

Sample 1	Sample 2	Assignments
605 s	604 s	ν_4 PO_4^{3-} bending
781 vw		C–C stretch
872 w	872 w	ν_3 CO_3
1038 vvs br	1031 vvs br	ν_3 PO_4^{3-} stretch ν_1 CO_3^{2-}
1316 w		C–C vibr.
1419 m	1416 w	$\nu_3 CO_3$
1469 m	1468 m	$\nu_3 CO_3$
	1550 m	C=C, $\nu_3 CO_3$
1651 m	1663 m	OH deformation ν(C=O)
	1995 vw	CO vibrations
2800 sh	2800 sh	ν (CH$_3$) asym.
3429 sbr	3422 sbr	ν OH stretch
3738 sh		

Fig. 2. FTIR spectrum of the sample 2, in the range 400–4000 cm^{-1}.
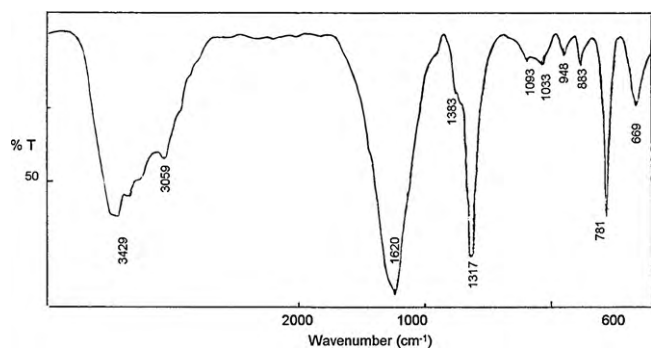
Fig. 3. FTIR spectrum of the sample 3, in the range 400–4000 cm^{-1}.

Table 3
IR spectral data (cm^{-1}) of urinary stone sample 3.

Sample 3	Assignments
669 w	ν_4 CO_3^{2-}
781 s	ν_4 CO_3^{2-}
883 vw	ν_2 CO_3^{2-}
949 vw	ν_1 CO_3^{2-}
1034 vw	ν_1 CO_3^{2-}
1093 vw	ν_1 CO_3^{2-}
1317 s	C–O vibr.
1383 ws	ν_3 CO_3^{2-} stretch
1620 s	δ OH
3059 sh	C=O stretch and overtone
3263 sh	ν O–H stretch
3336 sh	
3429 s	ν O–H stretch

vw—very weak; w—weak; wbr—weak broad; m—medium; vvw—very very weak; sh—shoulder; ms—moderately strong; vvs—very very strong; s—strong.

An endothermic peak is observed at 109 °C corresponding to a weight loss of 6.5% as per the TG analysis of sample 1. The DSC curve of the sample in the present investigation shows an endothermic peak at 112 °C representing a phase change in agreement with TGA/DTA data. An endothermic peak is observed at 87 °C corresponding to a weight loss of 5% as per the TG analysis of sample 2. The DSC curve of this sample shows an endothermic peak at 92 °C represents a phase change. There is a weight loss of 5% observed

in the TG curve of sample 3 at temperature of 97 °C, probably due to the loss of water of crystallization. The DSC data also shows a peak at around 92 °C. The initial weight loss from sample 1 (6.5%) indicates release of CO_2 upon heating and in other samples the weight loss due to CO_2 is only 5% [18]. This result further confirms our IR observation that amount of carbonation is less in samples 2 and 3 as compared to that of sample 1. The relatively low temperature (87 °C) of release of CO_2 from the sample 2 suggests that CO_2 groups are weakly bound to OH sites in agreement with IR observations.

The scanning electron micrographs of the samples under investigation are shown in Fig. 4. The rough and irregular granular type surface morphology is observed from the SEM micrographs of all the samples. But granular size is more in sample 1, and is less in sample 2 and shape of granules are different from that of sample 1. Further, sample 3 are also shows some morphological difference as compared to that of samples 1 and 2. These morphological differences in samples are quite expected since these crystals are having different chemical composition, crystalline structure and growth environment. Phosphate is one of the bases of the DNA and microorganism like *E. coli* strongly reduce urinary citrate and increase urease-induced calcium phosphate crystallization [17]. These microorganisms also help the biomineralisation of amorphous calcium carbonate in urinary system [23]. Usually the growth of a urinary calculus occurs around an initially formed nucleus. Some calculi comprise a single component, but the majorities have 'mixed' structure, showing variations in composition from the core to the surface. The large number of possible stone components and the variability in their relative arrangements within a stone add to the structural complexity [1]. Nucleation and the rate of nucleation are important steps in the crystallization process and are also important in determining its size and morphology of the crystals. Nucleation rate, growth and agglomeration depend on the specific conditions like molar concentrations, pH, temperature, etc. in a biological crystallization system [12,24,25]. Apart from this different types of trace elements including Mg, Cd, Pb, Zn, Fe, etc., may also affect the crystallization process [14]. There seems to be no doubt that stone formation is predominantly governed by a fixed particle mechanism, in other words, development from crystals into stones occurs in a fixed state [18]. Further, the morphology and chemical composition of these crystals depend upon
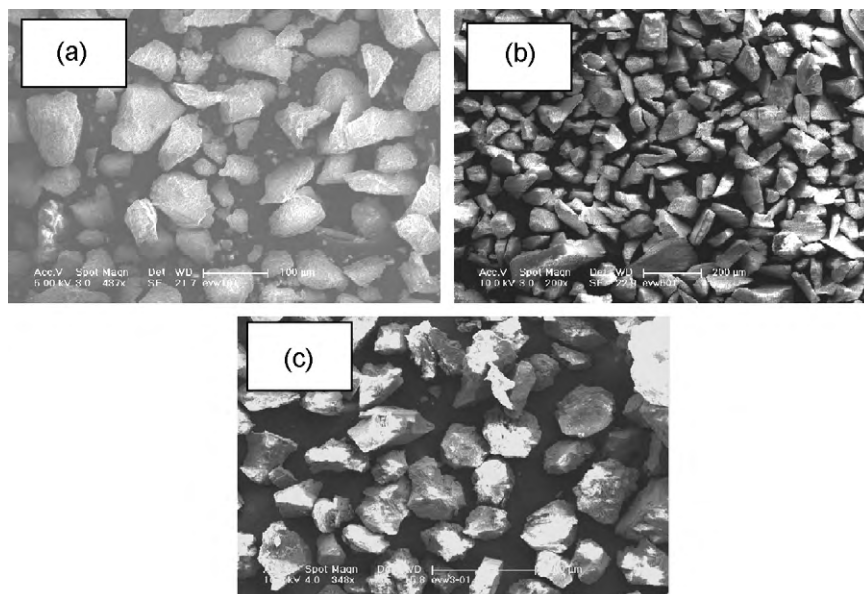

Fig. 4. Scanning electron micrographs of (a) sample 1 (calcium phosphate), (b) sample 2 (calcium phosphate hydroxide) and (c) sample 3 (sodium calcium carbonate).

time taken for super saturation and chemical reaction in mediums with varying pH. Once supersaturation condition inside the urinary bladder is achieved, the initial nucleation and formation of initial seedlings occur as a continuous process. Usually, after urination, the supersaturation condition may cease inside the urinary bladder. In most cases it may take several days for reaching another supersaturation condition inside the urinary bladder system for a favourable crystal growth condition. But, during this time probably, the previously grown crystalline seedlings are covered by a gelatinous mucinous layer (or a thin veil) of macromolecular or cellular (epithelial) material. This layer provides the framework for relatively undisturbed diffusion of the low-molecular-weight components of the crystal phase for further growth. This layer is amorphous in nature and contains different type of proteins and enriched with other carbonated species [13]. This carbonaceous component may be in sp^3 or sp^2 hybridised states or hydrogenated amorphous carbon (a C:H). This is evidenced by weak IR band at $1350\,cm^{-1}$ (a-C) in sample 1 and at $1550\,cm^{-1}$ ((a C:H).) in sample 2 and at 1317 (a-C) cm^{-1} in sample 3 [13,18]. The mucinous layer is continuously incorporated into the growing stone material thus becoming the well known stone matrix [21]. Supersaturation condition may again occur inside the urinary bladder, and this condition may be different from that of initial one at least several of the parameters like temperature, pH, or mineral concentration may vary. So, the secondary grown or deposits may be slightly varied in its morphology or shape and thus rule out the formation of defect and inclusion free single crystal. Thus obtained crystal may be an imperfect crystal usually an agglomeration (Fig. 4) of smaller crystallites with different morphology in agreement with the SEM micrographs.

4. Conclusions

The analysis indicates that the observed urinary stones are calcium phosphate, calcium phosphate hydroxide and sodium calcium carbonate. FTIR spectral investigations have revealed that carbonated species are occupied in PO_4 sites in calcium phosphate and carbonate content is occupied in OH sites in calcium phosphate hydroxide sample. Thermal studies of these samples also reveal the release of CO_2 upon heating with respect to amount of carbon content and bond strengths. Crystals with defects and irregular morphology are grown inside the urinary bladder due to natural variation in crystal growth conditions.

References

[1] M.T.M. Davidson, D.L. Batchelar, S. Velupillai1, J.D. Denstedt, I.A. Cunningham, Phys. Med. Biol. 50 (2005) 3907–3925.
[2] A.M. Ali, N.A.N. Raj, S. Kalainathan, P. Palanichamy, Mater. Lett. 62 (2008) 2351–2354.
[3] S.N. Kalkura, V.K. Vaidyan, M. Kanakavel, P. Ramasamy, J. Crystal Growth 132 (1993) 617–620.
[4] E.V. Wilson, M.J. Bushiri, V.K. Vaidyan, Perspectives in vibrational spectroscopy, in: V.K. Vaidyan, V.S. Jayakumar (Eds.), AIP Conference Proceedings 1075, New York, 2008, pp. 155–157.
[5] L.M. Al-Naam, Y. Baqir, H. Rasoul, L.P. Susan, M. Alkhaddar, Saudi Med. J. 8 (1987) 456–461.
[6] M.S. Modlin, Afr. Med. J. 59 (1981) 318–319.
[7] P.K. Grover, D.-S. Kim, R.L. Ryall, Mol. Med. 8 (4) (2002) 200–2009.
[8] JCPDS-International Centre for Diffraction Data (1997).
[9] K. Nakamoto, Infrared and Raman Spectra of Inorganic and Coordination Compounds—Part A, 5th ed., Wiley Interscience, New York, 1997.
[10] M.J. Bushiri, C.J. Antony, A. Aatiq, J. Phys. Chem. Solids 69 (2008) 1985–1989.
[11] J.A. Dean, The Analytical Chemistry Handbook, McGraw Hill, Inc., New York, 1995.
[12] P. Sundaramoorthi, S. Kalainathan, Biochem. Eng. J. 35 (2007) 244–249.
[13] L. Estepa, M. Daudon, Biospectroscopy 3 (1997) 347–355.
[14] T.K. Anee, M. Palanichamy, M. Ashok, N. Meenakshi Sundaram, S. Narayana Kalkura, Mater. Lett. 58 (2004) 478–482.
[15] K.-H. Chen, W.-T. Cheng, M.-J. Li, S.-Y. Lin, Graefe's Arch. Clin. Exp. Ophthalmol. 244 (2006) 407–410.
[16] J.V. Rau, S. Nunziante Cesaro, D. Ferro, S.M. Barinov, I.V. Fadeeva, J. Biomed. Mater. Res. Part B: Appl. Biomater. 71B (2004) 441–447.
[17] X. Carpentier, M. Daudon, O. Traxer, P. Jungers, A. Mazouyes, G. Matzen, E. Véron, D. Bazin, Urology 73 (2009) 968–975.
[18] A. Antonakos, E. Liarokapis, T. Leventouri, Biomaterials 28 (2007) 3043–3054.
[19] L. Addadi, S. Raz, S. Weiner, Adv. Mater. 15 (2003) 959–970.
[20] R.L. Frost, W.N. Martens, L. Rintoul, E. Mahmutagic, J.T. Kloprogge, J. Raman Spectrosc. 33 (2002) 252–259.
[21] W. Achilles, World J. Urol. I5 (1997) 244–251.
[22] C. Rey, V. Renugopalakrishnan, B. Collins, M.J. Glimcher, Calcif. Tissue Int. 49 (1991) 251–258.
[23] V.R. Phoenix, K.O. Konhauser, Geobiology 6 (2008) 303–308.
[24] V. Thongboonkerd, T. Semangoen, S. Chutipongtanate, Clin. Chim. Acta 367 (2006) 120–131.
[25] D.R. Basavaraj, C.S. Biyani, A.J. Browning, J.J. Cartledge, EAU-EBU Update Series 5 (2007) 126–136.